NOAA Technical Memorandum OAR PMEL-121

ATLAS Module Temperature Bias Due to Solar Heating

P.N. A'Hearn[1], H.P. Freitag[2] and M.J. McPhaden[2]

[1]Joint Institute for the Study of the Atmosphere and Ocean (JISAO)
University of Washington
Box 351640
Seattle, WA 98195

[2]Pacific Marine Environmental Laboratory
7600 Sand Point Way NE
Seattle, WA 98115

October 2002

Contribution 2486 from NOAA/Pacific Marine Environmental Laboratory
Contribution 939 from the Joint Institute for the Study of the Atmosphere and Ocean (JISAO)

NOTICE

Mention of a commercial company or product does not constitute an endorsement by NOAA/OAR. Use of information from this publication concerning proprietary products or the tests of such products for publicity or advertising purposes is not authorized.

Contribution No. 2486 from NOAA/Pacific Marine Environmental Laboratory
Contribution 939 from the Joint Institute for the Study of the Atmosphere and Ocean (JISAO)

For sale by the National Technical Information Service, 5285 Port Royal Road
Springfield, VA 22161

Contents

List of Figures

List of Tables

ATLAS Module Temperature Bias Due to Solar Heating

P.N. A'Hearn[1], H.P. Freitag[2] and M.J. McPhaden[2]

Abstract. Some near-surface temperature measurements from NextGeneration Autonomous Temperature Line Acquisition Systems (NX ATLAS) moorings between 1996 and 2001 have been found to be at times biased by solar heating. The bias is maximum near the sea surface around noon local time and has been observed at depths down to 75 m. Sea surface temperature sensors mounted immediately beneath the buoy at 1 m are not exposed to direct sunlight and thus not subject to similar solar heating. The bias is estimated to have a typical maximum of about 0.13°C at 20 m, the depth of the shallowest sensor on most moorings. Temperature sensors at 5 m and 10 m on some specially instrumented moorings may have larger biases. Modifications to the instrumentation and deployment procedures have reduced solar heating bias to 0.01°C or less. These improvements were first introduced in April 2000 and have been used on all moorings deployed since January 2001. The recovery of potentially biased instrumentation was completed in December 2001. A list of when and where data may be biased is given in the appendix.

1. Introduction

NX ATLAS moorings were developed by NOAA's Pacific Marine Environmental Laboratory (PMEL) to measure meteorological and oceanographic parameters in tropical latitudes. These moorings were developed in the mid-1990s and were first deployed in 1996 as part of the Tropical Atmosphere-Ocean (TAO) array (McPhaden *et al.*, 1998). They gradually replaced the original Standard ATLAS moorings in the array and occupied all locations by the end of 2001. NX ATLAS moorings have also been deployed in the Pilot Research Moored Array in the Tropical Atlantic (PIRATA) since its inception in 1997 (Servain *et al.*, 1998) and at other sites in the South China Sea and the North Pacific. Triangle Trans-Ocean Buoy Network (TRITON) moorings (http://www.jamstec.go.jp/jamstec/TRITON/), which replaced TAO moorings west of 165°E in late 2000, are maintained by the Japan Marine Science and Technology Center (JAMSTEC), and make measurements similar to those made by NX ATLAS moorings, using commercially available instruments. TRITON instrumentation is not discussed in this report.

It was discovered in 1998 that subsurface temperature measurements from NX ATLAS systems could be biased toward higher temperatures when exposed to sunlight. In this paper we describe the problem, and present solutions that have been developed to address it.

2. Sensor Description

NX ATLAS moorings use self-contained, internally recording subsurface sensor modules designed by PMEL's Engineering Development Division to record water properties. Each module can be configured to measure tempera-

[1]Joint Institute for the Study of the Atmosphere and Ocean (JISAO), University of Washington, Box 351640, Seattle, WA 98195

[2]NOAA/Pacific Marine Environmental Laboratory, 7600 Sand Point Way NE, Seattle, WA 98115

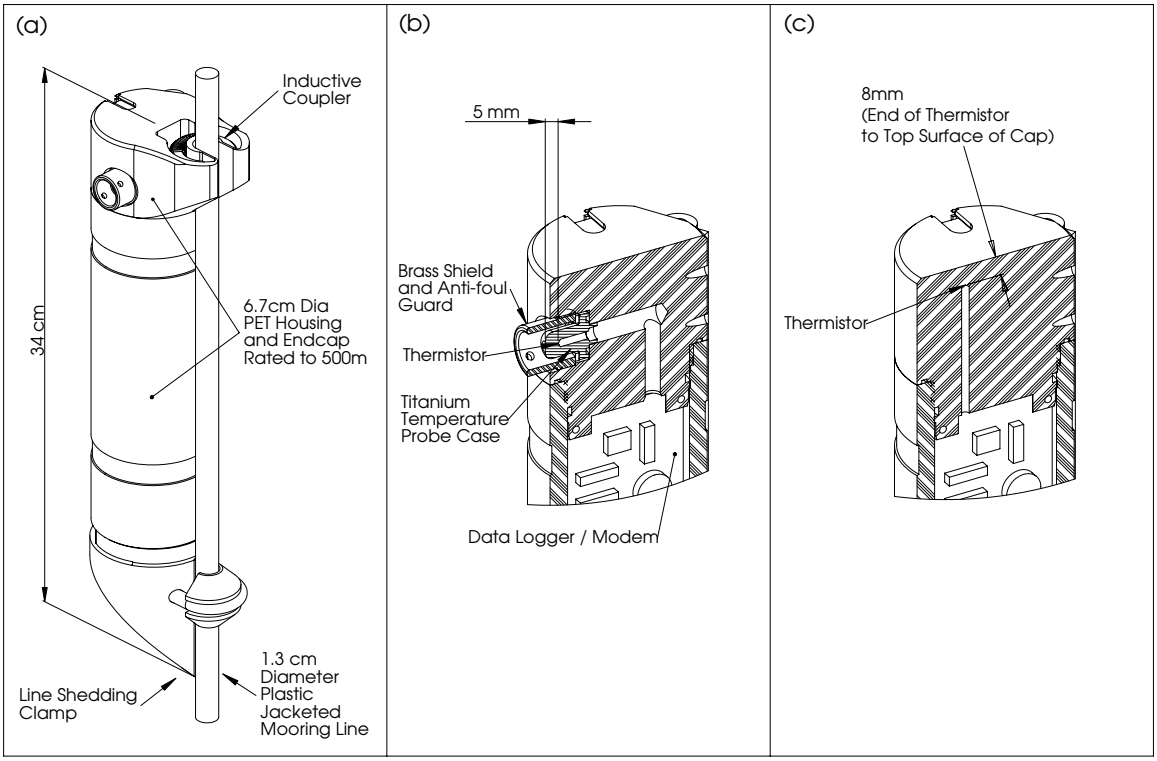

Figure 1: Schematic drawing (a) and cross section (b) of a "fast response" NX ATLAS module, and cross section (c) of the original NX ATLAS module.

ture alone, temperature and conductivity, or temperature and pressure. The pressure housing for the modules is machined from polyethylene terepthalate (PET) in two pieces: an end cap to which the sensors and circuitry are attached, and a hollow cylindrical pressure case (Fig. 1a).

As originally designed, the PET had a small amount of carbon black added for UV resistance, and was black to dark grey in color. The thermistor used to measure water temperature in these modules was 8 mm from the outside surface of the end cap at the end of a blind hole drilled from the interior (Fig. 1c). The module surface nearest to the thermistor was deployed toward the sea surface when attached to the mooring wire, and therefore this surface received the most direct sunlight. Later versions of the module design involved elimination of the carbon black from the PET to produce white cases, and end cap modifications to provide better exposure of the thermistor to sea water temperatures (Fig. 1b). These design modifications are described in more detail below.

3. Problem Description

In some cases, additional instruments are attached to ATLAS moorings for specific experiments. In one such case, SeaBird SBE-16's (Seacats) were attached to an NX ATLAS mooring at 8°N, 125°W in 1997. Temperature

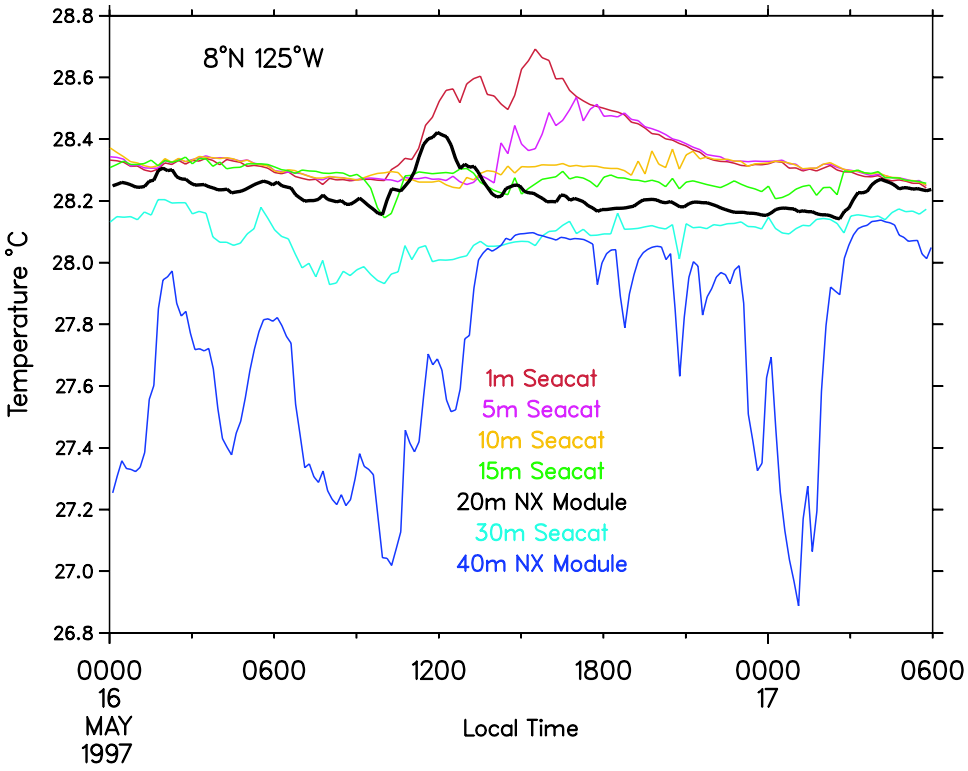

Figure 2: Temperature time series from 4 Seacats and 2 NX ATLAS modules deployed at 8°N, 125°W.

measurements from Seacats are believed to have minimal bias attributable to solar heating because the thermistor in these instruments is mounted in a thin titanium probe extending outside a titanium end cap, which provides rapid heat conductance to the surrounding water. Assuming that Seacat data are unbiased, differences between Seacat and NX ATLAS module temperatures may be used to quantify NX ATLAS module bias due to solar heating. In this case, NX ATLAS modules recorded significantly higher temperatures during daylight hours on some days. An example of solar heating was observed on 16 May 1997 when the temperature from an NX module at 20 m depth rose above temperatures from Seacats located between 5 m and 15 m (Fig. 2). At local noon the module temperature reached a maximum for the day and was 0.13°C above the temperature from a Seacat at 15 m. Real temperature inversions can occur in the ocean when salinity variations due to rainfall events or lateral intrusions stabilize the water column (e.g., McPhaden, 1985; Cronin and Kessler, 2002). The inversion shown in Fig. 2 and others like it in the NextGeneration temperature records are clearly instrumental in origin, however.

This diurnal temperature bias of near-surface NX modules is typically synchronous with shortwave solar radiation measured by Eppley PSP radiometers, which are mounted on some buoys. Recorded water temperature often peaks around local noon, rather than in the mid-afternoon as would be expected of typical warming of the water column. For example, on 11

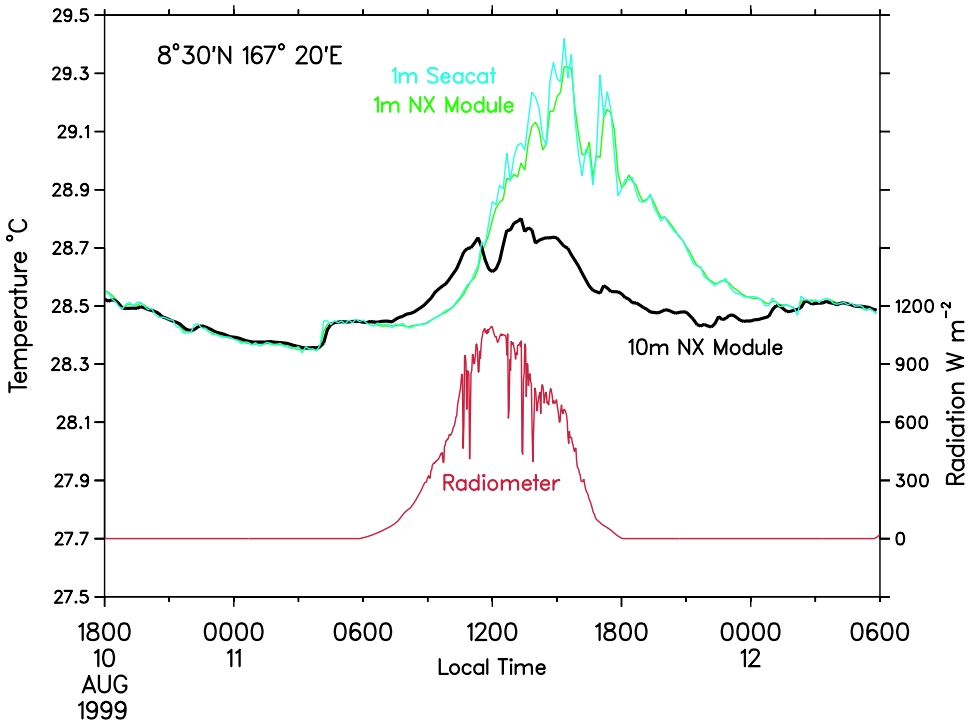

Figure 3: Temperature time series from a 1 m Seacat, NX Modules at 1 m and 10 m, and downwelling solar radiation from an Eppley PSP radiometer deployed near 8°N, 167°E.

August 1999 near 8°N, 167°E, the Sea Surface Temperature (SST) nominally measured at 1 m depth was highest around 1500 LMT. SST measurements are presumably unbiased due to shading by the surface buoy (see below). In contrast, the temperature from an NX module at 10 m began rising above the 1 m temperature at sunrise (0600 LMT, as indicated by the PSP) and reached a maximum bias of 0.15°C at 1100 LMT (Fig. 3). After 1100 LMT the 10 m temperature was less than that at 1 m. Nevertheless, some solar-heating bias undoubtedly remained (given the observed solar radiation), although it was smaller than the temperature gradient between 1 m and 10 m. Temperature bias similar to this has been observed at many sites in both TAO and PIRATA arrays at depths as great as 75 m.

The dip in 10 m temperature at noon (Fig. 3) is a feature commonly observed in other near-surface NX module time series biased by solar heating and is thought to be due to the buoy shading the module when the sun is directly overhead. Module SST measurements are not thought to be strongly affected by solar heating, as the instrument is mounted directly underneath the surface float, and is shaded from direct sunlight throughout the day. Differences between module SST and co-located Seacat measurements support this idea, in that they do not show diurnal bias similar to that observed deeper in the water column (Fig. 3). SST differences between the Seacat and ATLAS module are due to differences in sensor time constants and small-

scale temperature differences over the finite vertical distance (about 0.1 m) between instruments.

To estimate the relative heating of NX modules from sunlight, we apply tropical Pacific chlorophyll values (Strutton and Chavez, 2000) to the chlorophyll/light-attenuation relationship of Morel (1988), yielding light attenuation coefficients (K_{PAR}) for the tropical Pacific in the range 0.03 to 0.09 m^{-1}, typically being around 0.06 m^{-1}. Typical noon peak irradiance for cloudless days as measured from TAO array buoys instrumented with Eppley PSP radiometers is around 1100 W m^{-2}, approximately half of which (550 W m^{-2}) is in the visible frequency band (Siegel *et al.*, 1995; Mobley, 1994). Visible light, rather than ultraviolet or infrared, which are attenuated strongly in seawater, is assumed to be the source of the heating. Assuming a worst-case scenario of low chlorophyll levels (K_{PAR} = 0.03 m^{-1}), a sea surface albedo of 0.03 (typical of tropical, clear-sky conditions near noon, Payne, 1972), no shadowing by the surface buoy, and only downwelling light, the upper bounds on solar radiation would be approximately 400 W m^{-2} at 10 m and 120 W m^{-2} at 50 m. The upward facing surface of the instrument pressure case has an area of 3.56×10^{-3} m^2. Assuming complete absorption of incoming light by the instrument, an upper bound for the estimate of radiant flux into the top of the instrument from solar radiation could be as much as 1.4 W at 10 m.

Modeling the measured temperature increase caused by this flux is relatively complicated and was not done for this study. We can however observe its effects, as illustrated by examples of peak temperature biases in the table below. Biases are typically largest around noon when the sun is near its zenith. They are generally lower in the morning and afternoon, and absent at night.

Table 1 lists peak bias for a number of modules, typically estimated by daytime comparison with measurements from a module 20 to 25 m deeper or shallower (but possibly still upwardly biased) for which nighttime temperatures indicated both modules were in a well-mixed layer. At shallow depths (where irradiance is greater) the water column typically heats up during the day. No attempt was made to account for such a vertical temperature gradient, as it is impossible to accurately separate solar heating of the module from actual increases in water temperature. Thus the heating bias could be overestimated or underestimated in some cases. The observed temperature biases listed in Table 1 are meant to give an idea of the range of values, but should not be considered uniformly applicable, as the bias is dependant on many factors such as cloudiness, sea surface albedo, solar elevation, and water clarity. As expected, the larger biases were nearest the surface. On the majority of ATLAS moorings the uppermost modules are placed at 20 m or 25 m. The largest bias observed from a 20 m black module was 0.13°C. Therefore, we conclude that 0.13°C represents a realistic upper bound on heating bias for modules typically deployed within the TAO and PIRATA mooring arrays. At depths of 50 m and below the observed bias in some instances approached the accuracy of the instrument, namely 0.01°C.

In a few special cases, modules have been placed shallower than 20 m. These include current meter moorings along the equator in the Pacific at

Table 1: Observed temperature biases, shown as peak values for a given day.

Mooring Name	Location (Latitude Longitude)	Depth (m)	Temperature Bias
PM121	10°N 95°W	5	0.42
PM121	10°N 95°W	10	0.20
PM092	8° 30′N 167° 20′E	10	0.15
PM016	8°N 125°W	20	0.13
PM035	0° 35°W	20	0.10
PM037	8°N 38°W	40	0.04
MOMMA	35°N 165°W	50	0.01
PM029	8°N 110°W	60	0.04
PM073	15°N 38°W	60	0.02
PM070	11°30′N 38°W	60	0.01
PM093	8°N 165°E	75	0.03
PMEL laboratory	—	—	0.08

110°W, 140°W, 170°W, and 165°E; two moorings deployed for about 6 weeks in the summer of 1999 near Kwajalein Island as part of the KWAJEX experiment (data from which are shown in Fig. 3); moorings deployed since fall of 1999 along 95°W for the Eastern Pacific Investigation of Climate Processes (EPIC); and three moorings deployed in the North Pacific between fall 1998 and summer 2000. The largest observed bias listed in Table 1 (0.42°C) from these shallower-than-normal modules was from a white module placed at 5 m on an EPIC mooring.

Daily averaged temperature, as reported in real-time data or derived from internally stored RAM data, will have a slight positive bias when this problem is present. Modeling the heating bias as the positive half of a sine wave for half the day produces a conservative upper bound on the daily mean bias of a factor of π^{-1}, or about one third, the daytime maximum. Thus heating bias of daily averaged temperature would be limited to about 0.04°C at typical module depths, and about 0.14°C for the shallower modules deployed in the special cases described above.

For NX ATLAS modules equipped with SeaBird conductivity cells, temperature bias will affect salinity measurements. Assuming that water within the conductivity cell is not significantly above ambient temperature, the error produced in the conductivity measurement from applying the biased thermistor temperature is insignificant (3.25×10^{-6} mS cm^{-1} °C^{-1}, based upon SeaBird calibration equations). However, salinity calculated using a temperature higher than that in the conductivity cell will be substantially biased downwards. At 30°C and 34 psu, a salinity error of –0.07 psu would result from a temperature bias of +0.1°C (Fig. 4). As for temperatures, daily averaged salinity bias would be roughly one third of the maximum daytime salinity bias.

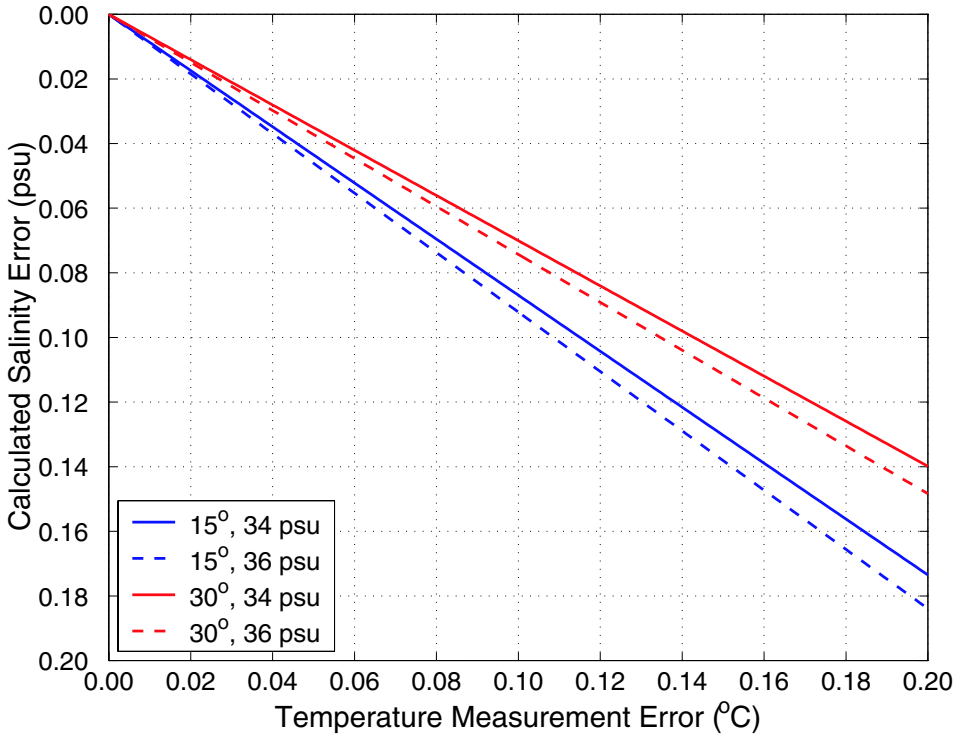

Figure 4: Salinity error (psu) due to temperature biases at temperatures of 15°C and 30°C and salinities of 34 psu and 36 psu.

4. Solutions

In response to this problem, near-surface (upper 50 m), black modules were attached on some moorings in an inverted, "top down" configuration beginning in September 1998. This reduced the heating of the end cap immediately surrounding the thermistor by orienting it away from direct sunlight. The quantitative effect of this change is difficult to calculate exactly, since it depends on several unknowns such as the thermal behavior of the entire pressure case, and irradiance as a function of direction. An empirical estimate of the effect of inverting the modules was obtained through PMEL laboratory tests. Incident radiation of order 120 W m^{-2} (as measured by a Biospherical Instruments QSP-200 radiometer) was produced by two 500 W floodlamps over a constant-temperature water bath. Mean temperature increases of 0.077°C were observed in upright modules exposed to the light, while mean increases in inverted modules were limited to 0.003°C. If similar results occur in the field, then mounting the instruments upside down should reduce the heating problem by approximately 96%. In this simple test, neither the lighting nor water flow in the bath were strictly uniform, therefore the results should be considered approximate.

While providing a rather simple solution to the module heating problem, inversion of the modules was not considered to be completely satisfactory, because the modules were more susceptible to being caught on fishing line

or nets when inverted. Beginning in 1999 new instruments were constructed using white PET pressure case material. As it was assumed that module heating would be reduced significantly in white modules, those initially deployed (beginning in July 1999) were oriented in an upright position. It was soon discovered that the change to white PET did not eliminate the problem of module heating. For example, the data from a white module at 10 m shown in Fig. 3 have a 0.15°C bias relative to the SST. In a laboratory test (similar to that described above) the temperature increase when exposed to light was 0.045°C on a white case compared to 0.062°C on a black case. Thus the substitution of white PET was much less effective than inverting the modules as a method of reducing solar heating bias. Beginning in February 2000, all modules in the upper 50 m (both black and white) were again deployed inverted. In January 2001 the depth of inverted modules was extended to 75 m.

Beginning in April 2000, modules were modified to place the thermistor inside a titanium probe which is exposed to sea water (Fig. 1b). The modification served two purposes; to decrease the thermal response time of the instruments (which improved salinity measurements[1]), and to decrease the solar heating effect. The modified instruments shade the thermistor from sunlight coming from directly above, as it is recessed within the side of the pressure case and is surrounded by a brass sleeve. Moreover, the titanium probe conducts heat more rapidly to the ambient water and thus is less prone to temperature bias. The effectiveness of these modifications is somewhat dependant on the speed at which water flows past the probe. Laboratory tests indicated a mean decrease in heating of 88% for upright, fast-response modules compared to the original black modules when upright. When inverted in the laboratory test, the mean heating in fast-response modules was limited to less than 0.002°C, a decrease of about 98% when compared to the original upright modules.

All modules deployed in the upper 75 m since January 2001 are fast-response modules. In addition, all new end caps and pressure cases are constructed from white PET material, and all instruments deployed at 75 m or shallower are inverted on the mooring line. Slow-response modules have been modified to the fast-response, titanium thermistor probe, and those which have black end caps or pressure cases are deployed at depths below 100 m. This combination of improvements should reduce the heating problem to about 2% of the value seen in the original black modules, for maximum

[1]In addition to reducing solar-heating bias, the fast-response modules have the added benefit of more closely matched temperature and conductivity response times. The original modules with thermistors inside the PET end cap (Fig. 1c) had a temperature time constant (e^{-1}) of order 800 s. The fast-response modules have a temperature time constant of order 30 s. The in situ time response of the conductivity sensor is strongly dependant upon mooring motion and ocean currents, which force sea water through the cell. PMEL-designed anti-foulant attachments to the conductivity cells were purposely constructed to slow the flow of water through the cell in order to extend the effective life of the anti-foulant and to better match the temperature and conductivity time response. Laboratory experiments indicate that in the presence of 2.7 m high waves of 7.5 s period, the time constant of the conductivity cell is of the same order as the fast-response temperature sensor (30 s).

daytime biases of ∼0.01°C or less for modules deployed at 5 m or deeper in the water column.

5. Summary

Measurements of high-resolution (10-min sample rate), near-surface temperature on NX ATLAS buoys deployed at standard depths (20 m and deeper) in the TAO and PIRATA Arrays may have positive daytime biases up to 0.13°C due to solar heating. These modules were first introduced into the TAO Array in 1996. The magnitude of the problem is proportional to incident solar radiation, and therefore greatest at shallow depths (but not SST measurements due to shading by the buoy), under clear skies, and in clear water conditions. Efforts to reduce the bias were begun in September 1998 by inverting the module orientation. Later improvements included changing to white case material and improving the thermistor mounting system. Instruments deployed in 2001 and thereafter are of the modified type. Solar heating, while potentially present in these new modules, should be less than 0.010°C, which is the accuracy of the instrument.

No corrections have been made to NX ATLAS data which are potentially biased due to solar heating. For standard deployment depths, data from NX ATLAS moorings deployed before 1999 have the greatest potential for solar heating bias. Between July 1999 and April 2000, upright modules were deployed at some mooring sites shallower than the 20 m standard depth, during which period a worst case bias of 0.42°C was observed. Thereafter, all modules in the upper 50 m (later 75 m) were inverted. Details on the color, orientation, and time response of near-surface modules deployed before the introduction of inverted, fast-response modules are listed in the appendix.

General criteria for determining the potential for data biased by solar heating are:

1. Near surface modules were biased more than deeper modules.
2. Black, slow-response, upward modules were most biased.
3. Black modules were biased more than white modules.
4. Upright modules were biased more than inverted modules.
5. Fast response, inverted modules (of either color) are the least biased.

Laboratory tests indicated the following reductions in the bias relative to the original black, slow response, upwardly oriented modules:

White, slow-response, upward	∼27%
White, fast-response, upward	∼88%
Black, slow-response, inverted	∼96%
White, fast-response, inverted	∼98%

White, fast-response, inverted modules are not included in the appendix, as they represent the present ATLAS configuration and are considered to

be effectively unbiased. Black, fast-response, inverted modules are likewise omitted from the appendix, as it is assumed their performance is similar if not equal to white, fast-response, inverted modules, and better than black, slow-response, inverted modules which had a 96% reduction in bias. Black, slow-response, inverted modules are included in the appendix because they are not the type and orientation of module used at present, although they have substantially less bias than upright modules.

Due to the diurnal nature of the solar bias, daily mean bias values from NX modules should be about one third the peak bias observed in the 10-min data. For the bulk of TAO and PIRATA moorings, with the first subsurface temperature module located at 20 m depth, this bias should be about 0.04°C or less. On specially instrumented moorings with modules placed between 5 m and 10 m, daily mean biases could be as large as 0.13°C.

Standard ATLAS moorings, used from the inception of the array in 1984 until retired in 2001, reported daily means only. Temperature sensors on these moorings were constructed of grey (rather than black) plastic and the thermistors were not near the upper surface of the instrument or in direct contact with the case. Thus, bias due to solar heating is expected to be less than that of NX modules and the potential bias due to solar heating in Standard ATLAS daily-mean measurements would be substantially lower than their accuracy of 0.09°C (Freitag *et al.*, 1994).

6. Acknowledgments

We would like to thank Chris Meinig, Engineering Development Division Leader at PMEL, for the design and development of improvements to the NX temperature modules. Also, special thanks to Meghan Cronin for comments on an earlier version of this report. This work was supported by NOAA's Office of Oceanic and Atmospheric Research, and by the Joint Institute for the Study of the Atmosphere and Ocean (JISAO under NOAA Cooperative Agreement No. NA17RJ11232, Contribution #939. This is PMEL Contribution #2486.

7. References

Cronin, M.F., and W.S. Kessler (2002): Seasonal and interannual modulation of mixed layer variability at 0°, 110°W. *Deep-Sea Res., 49*(1), 1–7.

Freitag, H.P., Y. Feng, L.J. Mangum, M.P. McPhaden, J. Neander, and L.D. Stratton (1994): Calibration procedures and instrumental accuracy estimates of TAO temperature, relative humidity and radiation measurements. NOAA Tech. Memo. ERL PMEL-104, 32 pp.

McPhaden, M.J. (1985): Fine-structure variability observed in CTD measurements from the central equatorial Pacific. *J. Geophys. Res., 90,* 11,726–11,740.

McPhaden, M.J., A.J. Busalacchi, R. Cheney, J.R. Donguy, K.S. Gage, D. Halpern, M. Ji, P. Julian, G. Meyers, G.T. Mitchum, P.P. Niiler, J. Picaut, R.W. Reynolds, N. Smith, and K. Takeuchi (1998): The Tropical Ocean-Global Atmosphere (TOGA) observing system: A decade of progress. *J. Geophys. Res., 103,* 14,169–14,240.

Mobley, C.D. (1994): *Light and Water; Radiative Transfer in Natural Waters.* Academic Press, 592 pp.

Morel, A. (1988): Optical modeling of the upper ocean in relation to its biogenous content (Case I Waters). *J. Geophys. Res, 93,* 10,749–10,768.

Payne, R.E. (1972): Albedo of the sea surface. *J. Atmos. Sci., 29,* 959–970.

Servain, J., A.J. Busalacchi, M.J. McPhaden, A.D. Moura, G. Reverdin, M. Vianna, and S.E. Zebiak (1998): A Pilot Research Moored Array in the Tropical Atlantic (PIRATA). *Bull. Am. Meteorol. Soc., 79,* 2019–2031.

Siegel, D.A., J.C. Ohlmann, L. Washburn, R.R. Bidigare, C.T. Nosee, E. Fields, and Y. Zhou (1995): Solar radiation, phytoplankton pigments, and the radiant heating of the equatorial Pacific warm pool. *J. Geophys. Res., 100*(C3), 4485–4891.

Strutton, P.G., and F.P. Chavez (2000): Primary productivity in the equatorial Pacific during the 1997–98 El Niño. *J. Geophys. Res, 105,* 26,089–26,101.

Appendix

Mooring sensor information

PIRATA (Eastern Atlantic)

Latitude Longitude (Degrees)	Mooring Name	Deployment Date (Mo/Da/Yr)	Recovery Date (Mo/Da/Yr)	Depth (m)	Color Black/White	Response Slow/Fast	Orientation Upright/Inverted
0°, 0°	PM038	02/01/98	11/08/98	20	B	S	U
				40	B	S	U
				60	B	S	U
	PM066	11/04/98	01/12/99	20	B	S	*
				40	B	S	*
				60	B	S	*
	PM160	08/08/00	12/10/01	20	W	F	*
				40	W	F	*
				60	W	F	*
2°N, 10°W	PM111	11/01/99	03/06/00	20	*	S	*
				40	*	S	*
				60	*	S	*
	PM133	03/10/00	07/30/00	20	W	S	I
				40	W	S	I
				60	B	S	U
0°, 10°W	PM031	09/14/97	11/20/97	25	B	S	U
				50	B	S	U
				75	B	S	U
	PM068	01/28/99	03/11/00	20	B	S	I
				40	B	S	I
				60	B	S	U
	PM134	03/11/00	11/22/00	20	W	S	I
				40	W	S	I
				60	B	S	I
2°S, 10°W	PM110	11/02/99	03/12/00	20	*	S	*
				40	*	S	*
				60	B	S	*
5°S, 10°W	PM067	01/27/99	03/13/00	20	B	S	I
				40	B	S	I
				60	B	S	U
	PM135	03/14/00	11/25/00	20	W	S	I
				40	W	S	I
				60	*	S	I
10°S, 10°W	PM030	09/10/97	11/04/98	20	B	S	U
				40	B	S	U
				60	B	S	U
	PM063	11/04/98	10/30/99	20	B	S	*
				40	B	S	*
				60	B	S	*
	PM109	10/30/99	11/27/00	20	*	S	U
				40	B	S	U
				60	B	S	U

* = unknown

PIRATA (Western Atlantic)

Latitude Longitude (Degrees)	Mooring Name	Deployment Date (Mo/Da/Yr)	Recovery Date (Mo/Da/Yr)	Depth (m)	Color Black/White	Response Slow/Fast	Orientation Upright/Inverted
0°, 23°W	PM078	03/06/99	02/23/00	20	B	S	I
				40	B	S	I
				60	B	S	U
	PM128	02/24/00	05/07/01	20	W	S	I
				40	W	S	I
				60	W	S	U
0°, 35°W	PM035	01/21/98	02/23/99	20	B	S	U
				40	B	S	U
				60	B	S	U
	PM077	02/23/99	03/28/00	20	B	S	I
				40	B	S	I
				60	B	S	U
	PM140	03/28/00	05/03/01	20	W	S	I
				40	W	S	I
				60	W	S	U
15°N, 38°W	PM036	01/27/98	02/05/99	20	B	S	U
				40	B	S	U
				60	B	S	U
	PM073	02/05/99	03/14/00	20	B	S	I
				40	B	S	I
				60	B	S	U
	PM136	03/15/00	04/16/01	20	W	S	I
				40	W	S	I
				60	B	S	U
11°30′N, 38°W	PM070	02/03/99	03/16/00	20	B	S	I
				40	B	S	I
				60	B	S	U
	PM137	03/16/00	01/15/01	20	W	S	I
				40	W	S	I
				60	B	S	U
8°N, 38°W	PM037	01/30/98	02/08/99	20	B	S	U
				40	B	S	U
				60	B	S	U
	PM074	02/08/99	03/18/00	20	B	S	I
				40	B	S	I
				60	B	S	U
	PM138	03/18/00	04/19/01	20	W	S	I
				40	W	S	I
				60	B	S	U
4°N, 38°W	PM076	02/20/99	03/19/00	20	B	S	I
				40	B	S	I
				60	B	S	U
	PM139	03/19/00	04/20/01	20	W	S	I
				40	W	S	I
				60	B	S	U

TAO (95°W)

Latitude Longitude (Degrees)	Mooring Name	Deployment Date (Mo/Da/Yr)	Recovery Date (Mo/Da/Yr)	Depth (m)	Color Black/White	Response Slow/Fast	Orientation Upright/Inverted
12°N, 95°W	PM123	12/02/99	04/20/00	5	W	S	U
				10	W	S	U
				20	W	S	U
				40	W	S	U
				60	B	S	U
10°N, 95°W	PM122A	12/01/99	04/21/00	5	W	S	U
				10	W	S	U
				20	W	S	U
				40	W	S	U
				60	B	S	U
	PM122B	04/21/00	11/11/00	60	B	S	U
8°N, 95°W	PM028	08/05/97	11/10/98	20	B	S	U
				40	B	S	U
				60	B	S	U
	PM121A	11/30/99	04/23/00	5	W	S	U
				10	W	S	U
				20	W	S	U
				40	W	S	U
				60	B	S	U
	PM121B	04/23/00	11/10/00	60	B	S	U
5°N, 95°W	PM087	05/25/99	04/23/00	20	B	S	I
				40	B	S	I
				60	B	S	U
	PM181	11/09/00	11/23/01	60	W	F	U
3°30′N, 95°W	PM120	11/28/99	04/24/00	5	W	S	U
				10	W	S	U
				20	W	S	U
				40	W	S	U
				60	B	S	U
2°N, 95°W	PM065	11/08/98	07/20/99	20	B	S	U
				40	B	S	U
				60	B	S	U
	PM086	05/24/99	11/27/99	20	B	S	I
				40	B	S	I
				60	B	S	U
	PM118A	11/27/99	04/25/00	5	W	S	U
				10	W	S	U
				20	W	S	U
				40	W	S	U
				60	W	S	U
	PM118B	04/25/00	07/11/00	60	W	S	U

TAO (95°W cont.)

Latitude Longitude (Degrees)	Mooring Name	Deployment Date (Mo/Da/Yr)	Recovery Date (Mo/Da/Yr)	Depth (m)	Color Black/White	Response Slow/Fast	Orientation Upright/Inverted
0°, 95°W	PM064	11/06/98	05/22/99	20	B	S	U
				40	B	S	U
				60	B	S	U
	PM085	05/23/99	11/26/99	20	B	S	I
				40	B	S	I
				60	B	S	U
	PM117A	11/26/99	04/26/00	5	W	S	U
				10	W	S	U
				20	W	S	U
				40	W	S	U
				60	B	S	U
	PM117B	04/26/00	11/05/00	60	B	S	U
2°S, 95°W	PM116A	11/25/99	04/27/00	5	W	S	U
				10	W	S	U
				20	W	S	U
				40	W	S	U
				60	B	S	U
	PM116B	04/27/00	11/04/00	60	B	S	U
5°S, 95°W	PM084	05/20/99	04/28/00	20	B	S	I
				40	B	S	I
				60	B	S	U
8°S, 95°W	PM007	05/13/96	08/11/97	20	B	S	U
				40	B	S	U
				60	B	S	U
	PM115A	11/23/99	04/30/00	5	W	S	U
				10	W	S	U
				20	W	S	U
				40	W	S	U
				60	B	S	U
	PM115B	04/30/00	11/12/00	60	B	S	U

TAO (110°W)

Latitude Longitude (Degrees)	Mooring Name	Deployment Date (Mo/Da/Yr)	Recovery Date (Mo/Da/Yr)	Depth (m)	Color Black/White	Response Slow/Fast	Orientation Upright/Inverted
8°N, 110°W	PM029	08/22/97	10/23/98	20	B	S	U
				40	B	S	U
				60	B	S	U
	PM112A	11/11/99	05/12/00	20	*	S	U
				40	W	S	U
				60	*	S	U
	PM112B	05/12/00	10/21/00	60	*	S	U
2°N, 110°W	PM113A	11/13/99	05/09/00	20	*	S	U
				40	*	S	U
				60	*	S	U
	PM113B	05/09/00	10/23/00	60	*	S	U
0°, 110°W	PM062	10/27/98	05/11/99	20	B	S	U
				40	B	S	U
				60	B	S	U
	PM083	05/11/99	11/15/99	10	B	S	U
				20	B	S	I
				25	B	S	U
				40	B	S	I
				60	B	S	U
	PM114	11/15/99	05/07/00	20	W	S	I
				40	W	S	I
				60	W	S	U
8°S, 110°W	PM008	05/16/96	08/15/97	20	B	S	U
				40	B	S	U
				60	B	S	U

* = unknown

TAO (125°W)

Latitude Longitude (Degrees)	Mooring Name	Deployment Date (Mo/Da/Yr)	Recovery Date (Mo/Da/Yr)	Depth (m)	Color Black/White	Response Slow/Fast	Orientation Upright/Inverted
8°N, 125°W	PM044	04/25/98	09/14/98	20	B	S	U
				40	B	S	U
				60	B	S	U
	PM107	10/06/99	02/24/00	20	B	S	*
				40	*	S	*
				60	*	S	*
	PM129	02/25/00	09/08/00	20	W	S	I
				40	W	S	I
				60	B	S	U
	PM161	09/08/00	02/07/01	60	W	F	U
5°N, 125°W	PM017	04/03/97	04/26/98	20	B	S	U
				40	B	S	U
				60	B	S	U
	PM045B	08/09/98	09/16/98	20	B	S	U
				40	B	S	U
				60	B	S	U
2°N, 125°W	PM075	02/13/99	10/02/99	20	B	S	*
				40	B	S	*
				60	B	S	U
	PM106	10/03/99	09/12/00	20	B	S	*
				40	B	S	*
				60	B	S	*
0°, 125°W	PM009	06/24/96	04/06/97	20	B	S	U
				40	B	S	U
				60	B	S	U
	PM018	04/08/97	04/28/98	20	B	S	U
				40	B	S	U
				60	B	S	U
	PM046	04/29/98	09/18/98	20	B	S	U
				40	B	S	U
				60	B	S	U
	PM058	09/18/98	10/01/99	20	B	S	I
				40	B	S	I
				60	B	S	U
	PM105	10/01/99	02/21/00	20	B	S	*
				40	W	S	*
				60	B	S	*
	PM127	02/21/00	02/04/01	20	W	S	I
				40	W	S	I
				60	B	S	U

* = unknown

TAO (140°W)

Latitude Longitude (Degrees)	Mooring Name	Deployment Date (Mo/Da/Yr)	Recovery Date (Mo/Da/Yr)	Depth (m)	Color Black/White	Response Slow/Fast	Orientation Upright/Inverted
9°N, 140°W	PM102	09/15/99	09/26/00	20	B	S	I
				40	B	S	I
				60	B	S	U
5°N, 140°W	PM061	10/01/98	01/31/99	20	B	S	I
				40	B	S	I
				60	B	S	U
	PM069B	09/17/99	02/09/00	20	B	S	*
				40	B	S	*
				60	B	S	U
	PM124	02/10/00	01/22/01	20	B	S	I
				40	W	S	I
				60	W	S	U
2°N, 140°W	PM060	09/30/98	02/03/99	20	B	S	I
				40	B	S	I
				60	B	S	U
	PM071	02/04/99	09/14/99	20	B	S	*
				40	B	S	*
				60	B	S	U
	PM103	09/18/99	02/11/00	20	B	S	I
				40	B	S	I
				60	B	S	U
	PM125	02/11/00	01/23/01	20	W	S	I
				40	W	S	I
				60	B	S	U
0°, 140°W	PM072	02/05/99	09/19/99	20	B	S	*
				40	B	S	*
				60	B	S	U
	PM104	09/21/99	02/12/00	20	*	S	*
				40	*	S	*
				60	*	S	*
	PM126	02/12/00	09/23/00	20	*	S	I
				40	*	S	I
				60	*	S	U

* = unknown

TAO (155°W, 170°W, 180°)

Latitude Longitude (Degrees)	Mooring Name	Deployment Date (Mo/Da/Yr)	Recovery Date (Mo/Da/Yr)	Depth (m)	Color Black/White	Response Slow/Fast	Orientation Upright/Inverted
8°N, 155°W	PM148	06/19/00	06/02/01	25	W	S	I
				50	*	S	I
				75	*	S	I
2°N, 155°W	PM088	07/07/99	06/22/00	25	W	S	U
				50	W	S	U
				75	B	S	U
	PM149	06/22/00	06/06/01	25	W	S	I
				50	W	S	I
				75	*	S	I
0°, 155°W	PM108	10/27/99	10/21/00	25	W	S	U
				50	W	S	U
				75	B	S	U
2°S, 155°W	PM150	06/23/00	06/08/01	25	W	S	I
				50	W	S	I
				75	W	S	I
5°N, 170°W	PM013	07/26/96	05/26/97	25	B	S	U
				50	B	S	U
				75	B	S	U
	PM022	05/27/97	06/25/98	25	B	S	U
				50	B	S	U
				75	B	S	U
	PM050	06/26/98	07/22/99	25	B	S	U
				50	B	S	U
				75	B	S	U
	PM090	07/23/99	07/05/00	25	W	S	U
				50	W	S	U
				75	B	S	U
	PM152	07/06/00	06/20/01	25	W	S	I
				50	W	S	I
				75	*	S	I
2°N, 180°	PM011	06/29/96	06/24/97	25	B	S	U
				50	B	S	U
				75	B	S	U
	PM027	06/25/97	07/22/98	25	B	S	U
				50	B	S	U
				75	B	S	U
	PM056	07/23/98	07/25/99	25	B	S	U
				50	B	S	U
				75	B	S	U
	PM100	08/21/99	08/02/00	25	W	S	*
				50	W	S	*
				75	B	S	*
0°, 180°	PM119	11/28/99	11/30/00	25	W	S	U
				50	W	S	U
				75	B	S	U
	PM191	11/30/00	11/14/01	75	B	S	U
2°S, 180°	PM190	11/29/00	07/19/01	50	W	S	I
				75	B	S	U

* = unknown

TAO (KWAJEX)

Latitude Longitude (Degrees)	Mooring Name	Deployment Date (Mo/Da/Yr)	Recovery Date (Mo/Da/Yr)	Depth (m)	Color Black/White	Response Slow/Fast	Orientation Upright/Inverted
8°N, 168°E	PM091	07/29/99	09/14/99	5	W	S	U
				10	W	S	U
				20	W	S	U
				40	W	S	U
				60	B	S	U
8°N, 167°E	PM092	07/30/99	09/13/99	5	W	S	U
				10	W	S	U
				20	W	S	U
				40	W	S	U
				60	B	S	U

TAO (165°E)

Latitude Longitude (Degrees)	Mooring Name	Deployment Date (Mo/Da/Yr)	Recovery Date (Mo/Da/Yr)	Depth (m)	Color Black/White	Response Slow/Fast	Orientation Upright/Inverted
8°N, 165°E	PM023	06/09/97	07/07/98	25	B	S	U
				50	B	S	I
				75	B	S	U
	PM051	07/08/98	08/05/99	25	B	S	U
				50	B	S	U
				75	B	S	U
	PM093	08/06/99	07/18/00	25	B	S	I
				50	B	S	I
				75	B	S	U
5°N, 165°E	PM024	06/11/97	07/09/98	25	B	S	U
				50	B	S	U
				75	B	S	U
	PM052	07/09/98	08/07/99	25	B	S	U
				50	B	S	U
				75	B	S	U
	PM094	08/07/99	07/19/00	25	W	S	U
				50	B	S	I
				75	B	S	U
	PM184	11/18/00	11/06/01	75	W	S	U
2°N, 165°E	PM032	01/06/98	03/20/99	25	B	S	U
				50	B	S	U
				75	B	S	U
	PM082	03/21/99	08/08/99	25	B	S	I
				50	B	S	I
				75	B	S	U
	PM095	08/09/99	02/27/00	25	B	S	I
				50	B	S	I
				75	B	S	U
	PM130	02/28/00	04/20/00	25	W	S	I
				50	W	S	U
				75	W	S	U

TAO (165°E cont.)

Latitude Longitude (Degrees)	Mooring Name	Deployment Date (Mo/Da/Yr)	Recovery Date (Mo/Da/Yr)	Depth (m)	Color Black/White	Response Slow/Fast	Orientation Upright/Inverted
0°, 165°E	PM081	03/20/99	08/10/99	25	B	S	I
				50	B	S	I
				75	B	S	U
	PM096	08/11/99	10/21/99	25	B	S	I
				50	B	S	I
				75	B	S	U
	PM131	02/29/00	07/22/00	25	W	S	I
				50	W	S	I
				75	W	S	U
	PM185	11/20/00	07/09/01	75	*	F	U
2°S, 165°E	PM025	06/15/97	07/11/98	25	B	S	U
				50	B	S	U
				75	B	S	U
	PM054	07/12/98	08/11/99	25	B	S	U
				50	B	S	U
				75	B	S	U
	PM097	08/12/99	07/23/00	25	B	S	I
				50	B	S	I
				75	B	S	U
5°S, 165°E	PM012	07/09/96	02/01/97	25	B	S	U
				50	B	S	U
				75	B	S	U
	PM034	01/10/98	03/13/99	25	B	S	U
				50	B	S	U
				75	B	S	U
	PM080	03/14/99	03/01/00	25	B	S	I
				50	B	S	I
				75	B	S	U
	PM132	03/02/00	11/21/00	25	W	S	I
				50	W	S	I
				75	W	S	I
	PM186	11/22/00	07/11/01	75	W	S	U
8°S, 165°E	PM026	06/17/97	07/14/98	25	B	S	U
				50	B	S	U
				75	B	S	U
	PM055	07/14/98	03/12/99	25	B	S	U
				50	B	S	U
				75	B	S	U
	PM079	03/13/99	07/26/00	25	B	S	I
				50	B	S	I
				75	B	S	U

TAO (156°E)

Latitude Longitude (Degrees)	Mooring Name	Deployment Date (Mo/Da/Yr)	Recovery Date (Mo/Da/Yr)	Depth (m)	Color Black/White	Response Slow/Fast	Orientation Upright/Inverted
0°, 156°E	PM057	08/21/98	10/06/99	25	B	S	U
				50	B	S	U
				75	B	S	U

* = unknown

South China Sea

Latitude Longitude (Degrees)	Mooring Name	Deployment Date (Mo/Da/Yr)	Recovery Date (Mo/Da/Yr)	Depth (m)	Color Black/White	Response Slow/Fast	Orientation Upright/Inverted
18°N, 116°E	PM020	04/27/97	04/09/98	25	B	S	U
				50	B	S	U
				75	B	S	U
	PM041	04/10/98	04/09/99	25	B	S	U
				50	B	S	U
				75	B	S	U
	PM098	08/19/99	05/07/00	25	*	S	*
				50	*	S	*
				75	B	S	*
15°N, 115°E	PM042	04/11/98	04/10/99	25	B	S	U
				50	B	S	U
				75	B	S	U
	PM099	08/20/99	05/04/00	25	*	S	*
				50	*	S	*
				75	*	S	*
13°N, 114°E	PM043	04/12/98	04/11/99	25	B	S	U
				50	B	S	U
				75	B	S	U
	PM101	08/21/99	05/05/00	25	*	S	*
				50	*	S	*
				75	*	S	*

North Pacific

Latitude Longitude (Degrees)	Mooring Name	Deployment Date (Mo/Da/Yr)	Recovery Date (Mo/Da/Yr)	Depth (m)	Color Black/White	Response Slow/Fast	Orientation Upright/Inverted
50°N, 145°W	PAPA1	09/28/98	06/08/99	6	B	S	U
				10	B	S	U
				15	B	S	U
				20	B	S	U
				30	B	S	U
				40	B	S	U
				50	B	S	U
				60	B	S	U
	PAPA2	10/10/99	08/12/00	5	W	S	U
				10	W	S	U
				15	*	S	U
				20	W	S	U
				30	B	S	U
				40	W	S	U
				50	*	S	U
				60	W	S	U
35°N, 165°W	MOMMA	09/28/99	10/01/00	5	W	S	U
				10	W	S	U
				15	W	S	U
				20	B	S	U
				30	W	S	U
				40	B	S	U
				50	W	S	U
				60	B	S	U

* = unknown